



UNIVERSITI PUTRA MALAYSIA

***BLACK PHOSPHORUS/POLYDIMETHYLSILOXANE COATED
MICROFIBER SATURABLE ABSORBER FOR ULTRASHORT PULSE
FIBER LASER***

NG ENG KHOON

FK 2022 87



**BLACK PHOSPHORUS/POLYDIMETHYLSILOXANE COATED
MICROFIBER SATURABLE ABSORBER FOR ULTRASHORT PULSE
FIBER LASER**

By

NG ENG KHOON

**Thesis Submitted to the School of Graduate Studies, Universiti Putra
Malaysia, in Fulfilment of the Requirements for the Degree of
Doctor of Philosophy**

October 2021

All material contained within the thesis, including without limitation text, logos, icons, photographs and all other artwork, is copyright material of Universiti Putra Malaysia unless otherwise stated. Use may be made of any material contained within the thesis for non-commercial purposes from the copyright holder. Commercial use of material may only be made with the express, prior, written permission of Universiti Putra Malaysia.

Copyright © Universiti Putra Malaysia



Abstract and thesis presented to the Senate of Universiti Putra Malaysia in fulfillment of the requirement for the degree of Doctor of Philosophy

**BLACK PHOSPHORUS/POLYDIMETHYLSILOXANE COATED
MICROFIBER SATURABLE ABSORBER FOR ULTRASHORT PULSE
FIBER LASER**

By

NG ENG KHOON

October 2021

Chair : Prof. Mohd Adzir bin Mahdi, PhD
Faculty : Engineering

Fiber lasers capable of generating ultrashort pulses have diverse applications in micromachining, medical science, and telecommunications. Ultrashort pulses generated from fiber lasers can be achieved through passive mode-locking *via* a saturable absorber (SA). Several black phosphorus (BP) fiber-based saturable absorbers have been reported with low damage thresholds, however, have poor repeatability for mass production due to uncontrollable deposition techniques. This research work focuses on a new technique to generate ultrashort pulses using optimized adiabatic tapered fiber saturable absorber with different dimensions of black phosphorus; vary from bulk to quantum dots.

The experimental work was initiated with the optimization of bulk BP polymer composite based saturable absorbers of different taper profiles in erbium-doped fiber ring laser cavity. The BP polymer composite was prepared by dispersing BP powders in tetrahydrofuran solvent then adding in polydimethylsiloxane (PDMS) to form composite. The sonicated BP was observed in chunky pieces within micrometers, proven by the scanning electron microscope morphological characterization. The characteristics of BP, PDMS, and BP/PDMS composite were analyzed through Raman spectroscopy, field emission scanning electron microscope, and ultraviolet-visible-near infrared absorption spectroscopy methods. A constant amount of BP polymer composite was deposited within the waist area of tapered fiber through spin coating method with optimized parameters; 4000 rpm for 6 minutes. The up/down transition and waist length were optimized with a waist diameter of 10 μm was chosen as the constant parameter. Based on the experimental findings, the optimum taper profile was 30 mm of up/down transition length and 1 mm of waist length, which resulted in transmission loss of 3.34 dB, saturation fluence of 21.56 $\mu\text{J}/\text{cm}^2$, and modulation depth of 3.14%. The fabricated BP/PDMS SA was integrated into a

ring cavity erbium-doped fiber laser (EDFL). By adjusting the polarization states of the circulating light in the cavity, the EDFL produced an optical spectrum with Kelly sidebands to prove the generation of conventional soliton (CS). The output pulse had a central wavelength of 1560.18 nm, 3-dB spectral width of 5.92 nm, pulse duration of 724 fs, repetition rate of 6.53 MHz, and time bandwidth product (TBP) of 0.53 showing the SA capable of generating ultrashort pulses.

Next, black phosphorus layers (BPLs) and black phosphorus quantum dots (BPQDs) were synthesized from bulk BP through liquid phase exfoliation method. The findings from high resolution transmission electron microscopy and atomic force microscopy suggested BPLs were in diameter range from 69 – 362 nm and thickness range of 42 – 62 nm. Whereas BPQDs displayed a lateral size of 2.92 ± 0.37 nm as analyzed from the TEM image. Then, BPLs/PDMS and BPQDs/PDMS composite SA were fabricated following the same procedure as implemented for BP/PDMS SA. These fabricated SAs were inserted into the same EDFL cavity to study their pulse performance characteristics. The transmission loss of BPLs/PDMS coated microfiber was 2.57 dB whereas BPQDs/PDMS composite coated microfiber was 2.12 dB at 1550 nm, respectively. The nonlinear absorption of BPLs/PDMS composite coated microfiber possesses saturation fluence of $9.22 \mu\text{J}/\text{cm}^2$, modulation depth of 3.5%, and two-photon absorption (TPA) of $5.3 \times 10^{-3} \text{ cm}^2/\mu\text{J}$ while the BPQDs/PDMS coated microfiber exhibited saturation fluence of $18.47 \mu\text{J}/\text{cm}^2$, modulation depth of 2.12%, and TPA coefficient of $9.1 \times 10^{-3} \text{ cm}^2/\mu\text{J}$. The nonlinear optical absorption response shows that due to different size of BPs, both SAs showed different TPA characteristics that caused CS to noise-like pulse (NLP) operation at different pump powers. In the CS operation, BPLs/PDMS composite SA generated 837 fs which was better in pulse duration compared to 1.11 ps of BPQDs/PDMS composite SA. Besides that, BPLs-SA had the lowest TBP value (0.39) among other structures BP-SAs which indicated the pulse was slightly chirped. However, in the NLP operation, BPQDs-SA showed shortest pulse generation at 152 fs due to strong TPA characteristic. Overall, the results validate the reliability of the proposed method to understand the effect of different BP/PDMS structures on microfiber based SAs for ultrashort pulse generation.

Abstrak tesis yang dikemukakan kepada Senat Universiti Putra Malaysia sebagai memenuhi keperluan untuk ijazah Doktor Falsafah

**PENYERAP TEPU GENTIAN MIKRO TERSALUT FOSFORUS
HITAM/POLIDIMETILSILOKSANA UNTUK LASER GENTIAN DENYUT
ULTRA PANTAS**

Oleh

NG ENG KHOON

Oktober 2021

Pengerusi : Prof. Mohd Adzir bin Mahdi, PhD
Fakulti : Kejuruteraan

Laser gentian yang mampu menghasilkan denyut ultra pantas mempunyai pelbagai aplikasi seperti pemesinan mikro, sains perubatan, dan telekomunikasi. Denyutan ultra pantas dari laser gentian boleh dicapai melalui penguncian mod pasif dengan penyerap tepu. Beberapa penyerap tepu berasaskan gentian fosforus hitam (BP) telah dilaporkan dengan ambang kerosakan yang rendah dan teknik pemendapan yang tidak terkawal menyebabkan kebolehlungan untuk pengeluaran besar-besaran yang rendah. Kerja penyelidikan ini menumpukan pada teknik baharu untuk menghasilkan denyutan ultra pantas menggunakan penyerap tepu gentian tirus adiabatik yang telah dioptimumkan dengan dimensi BP yang berbeza; dari pukal kepada titik kuantum.

Eksperimen dimulakan dengan pengoptimuman penyerap tepu berdasarkan komposit polimer BP bersaiz pukal dengan profil tirus yang berbeza dalam laser gentian terdop-erbium berskema cincin. Komposit polimer BP disediakan dengan mengsonikasi BP pukal dalam pelarut tetrahidrofur, kemudian ditambahkan polidimetilsiloksana (PDMS) ke dalam larutan. BP yang telah disonikasi mempunyai potongan kecil dalam skala mikrometer, dibuktikan dengan perincian morfologi mikroskop elektron pengimbas. Ciri-ciri komposit BP, PDMS dan BP/PDMS dianalisis menggunakan spektroskopi Raman, mikroskop elektron pengimbas pelepasan medan, dan kaedah spektroskopi penyerapan ultra violet-sinar tampak dan dekat infra merah. Komposit polimer BP yang berjisim sama didepositkan di kawasan pinggang gentian tirus melalui lapisan putaran pada 4000 putaran seminit untuk 6 minit. Peralihan naik/turun dan panjang pinggang telah dioptimumkan dengan diameter pinggang 10 μm dipilih sebagai parameter tetap. Dari penemuan eksperimen, profil tirus terbaik adalah 30 mm panjang peralihan ke atas/bawah dan 1 mm panjang pinggang, menghasilkan 3.34 dB kehilangan

transmisi, $21.56 \mu\text{J}/\text{cm}^2$ kelancaran tepu, dan 3.14% kedalaman modulasi. Penyerap tepu BP/PDMS telah diintegrasikan dalam laser gentian terdop-erbium berskema cincin. Dengan pelarasan polarisasi cahaya yang beredar dalam rongga, spektrum optik dengan jalur sisi Kelly membuktikan penghasilan soliton konvensional (CS). Denyut keluaran mempunyai panjang gelombang yang berpusat pada 1560.18 nm, 5.92 nm spektrum jalur lebar 3-dB, 724 fs jangka masa denyut, 6.53 MHz kadar pengulangan denyut, dan 0.53 jalur lebar masa (TBP).

Seterusnya, lapisan fosforus hitam (BPLs) dan titik kuantum fosforus hitam (BPQDs) telah disintesis dari BP pukal melalui kaedah pengelupasan fasa cecair. Penemuan dari mikroskop elektron transmisi beresolusi tinggi dan mikroskopi daya atom mencadangkan BPLs berada dalam julat diameter 69-362 nm dan julat ketebalan 42-62 nm. Manakala BPQDs menunjukkan ukuran lateral $2.92 \pm 0.37 \text{ nm}$ seperti yang telah dianalisis dari gambar TEM. Kemudian, penyerap tepu BPLs/PDMS dan BPQDs/PDMS komposit telah difabrikasi berdasarkan prosedur yang sama seperti yang dilaksanakan untuk penyerap tepu BP/PDMS. Penyerap tepu yang telah difabrikasi dimasukkan ke dalam rongga EDFL yang sama untuk mengkaji ciri-ciri prestasi denyut mereka. Kehilangan transmisi mikrofiber bersalut BPLs/PDMS dan BPQDs/PDMS adalah masing-masing 2.57 dB dan 2.12 dB pada 1550 nm. Penyerapan tidak linier mikrofiber bersalut komposit BPLs/PDMS mempunyai kelancaran tepu $9.22 \mu\text{J}/\text{cm}^2$, kedalaman modulasi 3.5%, dan pekali penyerapan dua foton (TPA) $5.3 \times 10^{-3} \text{ cm}^2/\mu\text{J}$ manakala mikrofiber bersalut BPQDs/PDMS mempamerkan kelancaran tepu $18.47 \mu\text{J}/\text{cm}^2$, kedalaman modulasi 2.12%, dan pekali TPA $9.1 \times 10^{-3} \text{ cm}^2/\mu\text{J}$. Tindak balas penyerapan optik tidak linier pada kedua-dua penyerap tepu menunjukkan ciri-ciri TPA yang berbeza disebabkan oleh dimensi BP yang berbeza. Hal ini menyebabkan operasi dari CS kepada NLP pada daya pam yang berbeza. Dalam operasi CS, penyerap tepu komposit BPLs/PDMS menghasilkan 837 fs durasi denyutan, yakni lebih baik berbanding 1.11 ps penyerap tepu komposit BPQDs/PDMS. Selain itu, penyerap tepu BPLs mempunyai nilai TBP terendah (0.41) berbanding struktur penyerap tepu BP yang lain, sebagai indikasi bahawa denyut sedikit terherot. Namun begitu, dalam operasi NLP, penyerap tepu BPQDs/PDMS telah menunjukkan penjanaan denyut terpendek pada 152 fs kerana ciri TPA yang kuat. Secara keseluruhan, dapatan mengesahkan kebolehpercayaan kaedah yang dicadangkan untuk memahami pengaruh struktur BP yang berbeza berdasarkan penyerap tepu mikrofiber untuk penjanaan denyut ultra pantas.

ACKNOWLEDGEMENTS

I would like to begin expressing my deepest gratitude to my supervisor, Prof. Mohd Adzir Mahdi for his guidance, knowledge sharing, and concern along my journey to finish the thesis. He has guided and advised me on how to be a critical thinking person. I also would like to give special thanks to my co-supervisors, Assoc. Prof. Dr. Muhammad Hafiz Abu Bakar and Dr. Josephine Liew Ying Chyi for their encouragement to work through challenges. To various people who had supported me during my work, thank you for your expertise, insights, and guidance. Among them, Dr. Lau Kuen Yao, Dr. Lee Han Kee, Norita Mohd Yusoff, and lab photonics members for training and providing equipment used in this study. In particular, I want to sincerely thank Chen Sim Yee for her continued advice and proofread throughout my writing. I would like to express my thanks to my friends and colleagues who also give some help either directly or indirectly in this project. Lastly, and most of all, my parents deserve special mention for their continual support and love throughout my life.

This thesis was submitted to the Senate of Universiti Putra Malaysia and has been accepted as fulfillment of the requirement for the degree of Doctor of Philosophy. The members of the Supervisory Committee were as follows:

Mohd Adzir bin Mahdi, PhD

Professor
Faculty of Engineering
Universiti Putra Malaysia
(Chairman)

Muhammad Hafiz bin Abu Bakar, PhD

Associate Professor
Faculty of Engineering
Universiti Putra Malaysia
(Member)

Josephine Liew Ying Chyi, PhD

Senior Lecturer
Faculty of Science
Universiti Putra Malaysia
(Member)

ZALILAH MOHD SHARIFF, PhD

Professor and Dean
School of Graduate Studies
Universiti Putra Malaysia

Date: 21 July 2022

Declaration by graduate student

I hereby confirm that:

- this thesis is my original work;
- quotations, illustrations and citations have been duly referenced;
- this thesis has not been submitted previously or concurrently for any other degree at any other institutions;
- intellectual property from the thesis and copyright of thesis are fully-owned by Universiti Putra Malaysia, as according to the Universiti Putra Malaysia (Research) Rules 2012;
- written permission must be obtained from supervisor and the office of Deputy Vice-Chancellor (Research and Innovation) before thesis is published (in the form of written, printed or in electronic form) including books, journals, modules, proceedings, popular writings, seminar papers, manuscripts, posters, reports, lecture notes, learning modules or any other materials as stated in the Universiti Putra Malaysia (Research) Rules 2012;
- there is no plagiarism or data falsification/fabrication in the thesis, and scholarly integrity is upheld as according to the Universiti Putra Malaysia (Graduate Studies) Rules 2003 (Revision 2012-2013) and the Universiti Putra Malaysia (Research) Rules 2012. The thesis has undergone plagiarism detection software.

Signature: _____ Date: _____

Name and Matric No.: Ng Eng Khoon , _____

Declaration by Members of Supervisory Committee

This is to confirm that:

- the research conducted and the writing of this thesis was under our supervision;
- supervision responsibilities as stated in the Universiti Putra Malaysia (Graduate Studies) Rules 2003 (Revision 2012-2013) are adhered to.

Signature: _____
Name of Chairman of
Supervisory
Committee: Prof. Dr. Mohd Adzir bin Mahdi

Signature: _____
Name of Member of
Supervisory
Committee: Assoc. Prof. Dr. Muhammad Hafiz bin Abu Bakar

Signature: _____
Name of Member of
Supervisory
Committee: Dr. Josephine Liew Ying Chyi

TABLE OF CONTENTS

	Page
ABSTRACT	i
ABSTRAK	iii
ACKNOWLEDGEMENTS	v
APPROVAL	vi
DECLARATION	viii
LIST OF TABLES	xiii
LIST OF FIGURES	xiv
LIST OF ABBREVIATIONS	xix
CHAPTER	
1 INTRODUCTION	1
1.1 Overview	1
1.2 Problem Statement and Motivation	2
1.3 Aim and Objective	3
1.4 Scope of Work	3
1.5 Organization of Thesis	4
2 LITERATURE REVIEW	5
2.1 Overview	5
2.2 Brief History of Fiber Optics and Lasers	5
2.3 Principles and Characteristics of Lasers	5
2.4 Development of Pulsed Fiber Lasers	7
2.4.1 Q-Switching	7
2.4.2 Gain Switching	8
2.4.3 Mode-Locking	9
2.5 Fundamental of Pulse Propagation in Optical Fibers	10
2.5.1 Dispersion	10
2.5.2 Nonlinearity	11
2.5.3 Soliton Formation in Mode-Locked Fiber Lasers	12
2.6 Passively Mode-Locked Fiber Lasers	13
2.6.1 Saturable Absorber Integration Schemes	16
2.7 Optical Properties of BP and Its Composite	17
2.8 Critical Review	19
2.9 Summary	21
3 BLACK PHOSPHORUS POLYMER COMPOSITE SATURABLE ABSORBER VIA EVANESCENT FIELD INTERACTION FOR ULTRASHORT PULSE GENERATION	22
3.1 Overview	22
3.2 Fabrication Process of BP-polymer Composite Coated Microfiber	22
3.2.1 Microfiber Fabrication and Its Optical Characterization	22

	3.2.2	Preparation of BP-Polymer Composite and Its Characterization	27
	3.2.3	Deposition of BP-Polymer Composite on Microfiber and Its Characterization	30
	3.3	Nonlinear Saturable Absorption Measurement	36
	3.4	Fiber Laser Passive Mode-Locking by BP/PDMS Composite Coated Microfibers	37
	3.5	Discussion	41
	3.6	Power Development and Stability Test of The Optimized BP/PDMS Microfiber SA	41
	3.7	Summary	43
4		MICROFIBER-BASED BLACK PHOSPHORUS FEW-LAYER AND QUANTUM DOT POLYMER COMPOSITE SATURABLE ABSORBER FOR MODE-LOCKED FIBER LASERS	44
	4.1	Overview	44
	4.2	Synthesis of BP Layers and Quantum Dots	44
	4.3	Preparation of BPL/PDMS and BPQDs/PDMS Composite	45
	4.4	Characterization of BPLs Exfoliated from BP Powders	45
	4.4.1	High-Resolution Transmission Electron Microscopy	45
	4.4.2	Atomic Force Microscope	46
	4.4.3	Raman Spectroscopy	47
	4.5	Characterization of BPQDs Exfoliated from BP Powders	48
	4.5.1	Transmission Electron Microscopy	48
	4.5.2	Photoluminescence Spectroscopy	49
	4.5.3	Raman and UV-VIS-NIR Spectroscopy	50
	4.6	Fabrication of BPLs and BPQDs Polymer Composite Devices and Their Characterizations	51
	4.7	Nonlinear Optical Absorption of BPLs and BPQDs Polymer Composite Devices	52
	4.8	Fiber Laser Passive Mode-Locking by BPLs/PDMS Composite Coated Microfibers	54
	4.8.1	Power Development and Stability Test of The BPLs/PDMS Microfiber SA	58
	4.9	Fiber Laser Passive Mode-Locking by BPQDs/PDMS Composite Coated Microfibers	60
	4.10	Discussion	66
	4.11	Summary	67
5		SUMMARY, CONCLUSION AND RECOMMENDATIONS FOR FUTURE RESEARCH	68

REFERENCES	71
APPENDICES	84
BIODATA OF STUDENT	94
LIST OF PUBLICATIONS	95



LIST OF TABLES

Table		Page
2.1	Performance Summary of Mode-Locked Lasers Based on Black Phosphorus Saturable Absorbers.	20
3.1	Taper Angles of Fibers with Different Transition Lengths.	24
3.2	Nonlinear Performance of Different Dimension of Microfibers Coated with BP/PDMS composite.	37
4.1	Pulse performance of CS and NLP operation for different structure BP-SA.	67
5.1	Pulse performance of CS and NLP operation for different structure BP-SA.	69

LIST OF FIGURES

Figure		Page
1.1	Scope of work.	3
2.1	A basic laser resonator setup.	6
2.2	Mechanism of laser formation.	6
2.3	Q-switch laser pulse formation.	8
2.4	Process of gain switching.	9
2.5	Schematic of a mode-locked ring laser cavity.	14
2.6	Incorporation schemes: (a) mirror (b) fiber ferrule (c) D-shaped fiber (d) microfiber (e) hollow-core photonic crystal fiber.	16
2.7	Process of saturable absorption of black phosphorus; (a) excitation and absorption incident light, (b) Fermi Dirac distribution form and (c) Pauli blocking and two-photon absorption.	19
3.1	Vytran automated glass processor workstation.	22
3.2	Schematic diagram of a microfiber.	23
3.3	Schematic for taper angle calculation.	23
3.4	Graphical user interface of Vytran GPX-3400 machine; (a) taper dimensions, and (b) taper parameters.	24
3.5	Fabricated of taper 15-1-15 dimensions;(a) captured image, and (b) output profile at scanning range of 45 mm.	25
3.6	Optical characterization of; (a) schematic experimental setup, (b) transmission of input signal and three samples of microfiber, (c) transmission loss of 15-1-15, (d) transmission loss of 20-1-20, (e) transmission loss of 25-1-25, and (f) transmission loss of 30-1-30.	26
3.7	Transmission loss of different transitions length of microfiber.	27

3.8	Preparation procedures; (a) mixing BP with THF, (b) dispersing BP, (c) addition of PDMS, (d) removing solvent, (e) addition of curing agent, and (f) degassing in vacuum condition.	28
3.9	Morphology structures of BP, (a) before, and (b) after sonication.	28
3.10	XRD pattern of dispersed BP crystals.	29
3.11	UV-VIS-NIR spectrum of sonicated bulk BP.	29
3.12	Raman spectra of BP, PDMS, and BP/PDMS composite.	30
3.13	Spin-coating of BP/PDMS composite on the microfiber.	31
3.14	Glass substrate of; (a) Kapton tape for creating step, and (b) hardened bridge of PDMS at constant rpm but different times.	31
3.15	Stylus contact profilometer of PDMS; (a) 1k rpm at 6min, (b) 3D mapping, and (c) 4k rpm at 6min.	32
3.16	PDMS film thickness with respect to spin coating speed and time.	33
3.17	Mass of BP/PDMS composite decorated on microfibers.	33
3.18	(a) Transmission loss of BP/PDMS composite decorated on different transtion length with fixed length and diameter, and (b) overall of transmission loss of BP/PDMS composite decorated on different dimension of microfibers.	34
3.19	Figure 3.19: Morphology of BP/PDMS composite coated microfiber; (a) cross-section view, film thickness for (b) right side, (c) left side, (d) a FESEM top view, EDX colors representation for (e) O, (f) C, (g) Si and (h) P where (i) EDX spectra of the FESEM image.	35
3.20	(a) Twin detector measurement setup, and (b) nonlinear responses of the coated sample.	36
3.21	Ring cavity mode-locked EDFL of; (a) experimental setup, and (b) schematic diagram.	38

3.22	Characterization of the performance EDFL by microfibers coated with BP/PDMS composite (a) optical spectrum, (b) autocorrelator trace, (c) oscilloscope trace, and (d) RF spectra.	39
3.23	Characterization of the performance EDFL by microfibers coated with BP/PDMS composite at maximum waist length; (a) optical spectrum, (b) autocorrelator trace, (c) oscilloscope trace, and (d) RF spectra.	40
3.24	Lasing performance of BP/PDMS composite decorated microfiber SAs with different dimensions; (a) modulation depth, and (b) pulse width.	41
3.25	Optimized BP/PDMS composite decorated microfiber SA of average output power and pulse energy.	42
3.26	Optimized BP/PDMS composite decorated microfiber SA stability test of (a) quantitative, (b) perspective view, and (c) top view.	42
4.1	Synthesis procedures; (a) grinding bulk BP, (b) probe sonication, (c) ultrasonic bath, (d) centrifugation, and (e) solvent exchange.	45
4.2	TEM images of BPLs with magnified Image A and Image B.	46
4.3	Characterizations of the BPLs; (a) AFM image, (b) height-profiling, and (c) the linear absorption spectrum. Inset: photograph of the BPLs solution.	47
4.4	Raman spectrum of BPLs, PDMS, and BPLs/PDMS.	48
4.5	Structural characterization of BPQDs; (a) TEM image of BQPDs, (b) statistical analysis on the sizes of 100 BPQDs measured from the TEM images, (c) enlarged TEM BQPDs with inset of HRTEM lattice fringe of BPQDs, (d) spacing measurements profile of BPQDs lattice fringes.	49
4.6	PL spectra of BPQDs in THF; (a) at different excitation wavelengths ranging from 330-350 nm, (b) PL emission spectrum at highest excitation by Gaussian fitting. Inset: photograph of the BPQDs solution under UV (360 nm).	50

4.7	Optical characterization and Raman analysis; (a) UV-VIS-NIR of BPQDs with inset photograph of BPQDs in THF solvent, and (b) Raman spectrum of BPQDs, PDMS and BPQDs/PDMS. Inset: enlarged of Raman spectrum at range of 300-800 cm^{-1} .	51
4.8	Transmission loss of BPLs/PDMS and BPQDs/PDMS composite devices.	52
4.9	Nonlinear optical absorption of; (a) BPLs/PDMS composite device, and (b) BPQDs/PDMS composite device.	53
4.10	Mode-locked EDFL spectrum evolution with respect to pump power.	54
4.11	Output characteristics of CS using BPLs/PDMS composite; (a) spectra at different pump powers, (b) spectrum at maximum pump power of 108.30 mW (c) pulse trains, (d) autocorrelation trace, and (e) RF spectrum at 60 MHz.	55
4.12	Output characteristics of NLP using BPLs/PDMS composite; (a) spectra at different pump power, (b) 3-dB bandwidth spectrum at maximum pump power, (c) autocorrelation trace of pedestal at different pump power, (d) spike at different pump power, (e) measured and fitted autocorrelation traces of pedestal, (f) measured and fitted autocorrelation traces of spike.	57
4.13	Oscilloscope and RF trace of NLP using BPLs/PDMS composite (a) pulse trains, and (b) RF spectrum at 60 MHz.	58
4.14	Average output power and pulse energy of CS and NLP operation against the manipulation of pump power.	58
4.15	Output stability of BPLs/PDMS composite SA mode-locked EDFL; (a) quantitative analysis (b) perspective view and (c) top view.	59
4.16	Output stability of NLP of BPLs/PDMS composite SA; (a) quantitative (b) perspective view, and (c) top view.	60
4.17	Mode-locked EDFL output spectrum evolution curve of BPQDs/PMDS SA.	61

4.18	Output characteristics of CS using BPQDs/PDMS composite with a pump power of 74.20 mW in experiment; (a) spectra at different pump powers, (b) spectrum of 3-dB and center wavelength at maximum pump power, (c) pulse trains, (d) autocorrelation trace, and (e) RF spectrum at 60 MHz.	62
4.19	Output characteristics of NLP using BPQDs/PDMS composite; (a) spectra at different pump powers, (b) 3-dB bandwidth spectrum at maximum pump power, (c) autocorrelation trace of pedestal at different pump powers, (d) spike at different pump powers, (e) measured and fitted autocorrelation traces of the pedestal (f) Gaussian fitting of spike.	63
4.20	Oscilloscope and RF trace of NLP using BPQDs/PDMS composite; (a) pulse trains (b) RF spectrum at 60 MHz.	64
4.21	Average output power and pulse energy of CS and NLP operation against the increased of pump power.	64
4.22	Output stability of BPQDs/PDMS composite SA mode locked EDFL; (a) quantitative analysis, (b) perspective view, and (c) top view.	65
4.23	Output stability of NLP of BPQDs/PDMS composite SA; (a) quantitative analysis, (b) perspective view and (c) top view.	66
5.1	Pulse performances of BP, BPLs and BPQDs SA.	70

LIST OF ABBREVIATIONS

AFM	Atomic Force Microscopy
ASE	Amplified Spontaneous Emission
BP	Black Phosphorus
BPLs	Black Phosphorus Layers
BPQDs	Black Phosphorus Quantum Dots
CNT	Carbon Nanotube
CS	Conventional Soliton
CVD	Chemical Vapor Deposition
CW	Continuous Wave
DMS	Dispersion-Managed Soliton
DS	Dissipative Soliton
EDX	Energy Dispersive X-ray Spectroscopy
FESEM	Field Emission Scanning Electron Microscope
FWHM	Full Width at Half Maximum
FWM	Four-Wave Mixing
GVD	Group Velocity Dispersion
HRTEM	High Resolution Transmission Electron Microscopy
ISO	Isolator
LD	Laser Diode
LPE	Liquid Phase Exfoliation
NALM	Nonlinear Amplifying Loop Mirror
NOLM	Nonlinear Optical Loop Mirror
NLO	Nonlinear Optical

NLP	Noise Like Pulse
NLSE	Nonlinear Schrodinger Equation
NPR	Nonlinear Polarization Rotation
OC	Optical Coupler
OPM	Optical Power Meter
OSA	Optical Spectrum Analyzer
PC	Polarization Controller
PCF	Photonic Crystal Fiber
PDI	Polarization-Dependent Isolator
PDL	Polarization Dependent Loss
PDMS	Polydimethylsiloxane
PL	Photoluminescence Spectroscopy
RBW	Resolution Bandwidth
RSAE	Reverse Saturable Absorption
SA	Saturable Absorber
SAE	Saturable Absorption Effect
SESAM	Semiconductor Saturable Absorber Mirror
SMFs	Single Mode Fibers
SNR	Signal to Noise Ratios
SPM	Self-Phase Modulation
TBP	Time Bandwidth Product
TEM	Transmission Electron Microscopy
THF	Tetrahydrofuran
TIR	Total Internal Reflection

TIs	Topological Insulators
TMDCs	Transition Metal Dichalcogenides
TPA	Two Photon Absorption
UV-Vis-NIR	Ultraviolet-Visible-near-IR
VBW	Video Bandwidth
VOA	Variable Optical Attenuator
WDM	Wavelength Division Multiplexer
XPM	Cross-Phase Modulation

CHAPTER 1

INTRODUCTION

1.1 Overview

Ultrashort pulse lasers have been making continuous technological advancements in diverse fields, such as medical, science and industrial applications. To name a few, applications for ultrashort pulse lasers include ophthalmology [1], bio-imaging [2], advanced micro-machining [3], quantum information processing [4], molecular spectroscopy [5], and nonlinear microscopy [6]. Some of the commercially available ultrafast lasers are titanium-sapphire, diode-pumped, and fiber lasers [7]. Out of those, fiber laser is considered as one of the most promising lasers that utilize rare-earth-doped fibers as optical gain medium. Besides, such laser is compact, flexible, and reliable, as well as exhibits excellent heat dissipation mechanism for the generation of ultrashort pulses.

Passive mode-locking technique is used to generate femtosecond pulses in ultrafast fiber laser system. This technique is usually realized with either free-space optical alignment or optical fiber laser cavities by employing either artificial or real saturable absorber (SA). Examples of artificial SA are nonlinear polarization rotation (NPR), nonlinear optical loop mirror (NOLM), and nonlinear amplifying loop mirror (NALM) in figure-of-eight configurations. Artificial SA usually deploys changing polarization state with a polarizer, such as the combination of a polarization-dependent isolator (PDI) and polarization controller (PC) for an NPR-based mode-locked fiber laser. However, artificial SA has the disadvantage of low environmental stability. The perturbation of light polarization state could experience a complex transient process before formation of soliton molecules, 23 times longer than carbon nanotubes (CNTs)-based mode-locked laser [8]. In addition, NPR-based SA shows stronger fluctuation of pumping strength, i.e., Q-switched instabilities are a typical phenomenon with longer nascent time generated before the formation of mode-locked laser, as compared to material-based SAs [9].

On the other hand, real SAs rely on material nonlinear saturable absorption properties to initiate and stabilize short pulses in various regimes. In particular, saturable absorption process depends on the imaginary part of the third-order nonlinearity of a material, whereas the real part indicates its nonlinear refractive index [10]. In addition, there are several properties that determine the quality of a material-based SA, such as direct bandgap tunability [11], nonlinear saturable absorption characteristics [12], and recovery time of a material that determines its power density for saturation [13], to name only a few. At the present time, the SA can be fabricated from different integration schemes by incorporating materials of saturable-absorption properties, such as III-V compound semiconductors [14], CNTs [15], graphene [16], topological insulators (TIs) [17], transition metal

dichalcogenides (TMDCs) [18], black phosphorus (BP) [19], MXene [20], antimonene [21], and bismuthene [22]. The major advantage of these materials is their relatively higher environmental stability than artificial SA.

In this research work, I focused on investigating different BP structures-based SA for generation of ultrashort pulses. BP was chosen due to its tunable bandgap, easy preparation for exfoliation into different structures, direct bandgap regardless thickness, and structure dependent saturable and reverse saturable absorption effect which are regarded remarkably important in ultrafast laser applications.

1.2 Problem Statement and Motivation

Up to date, BP has been reported as layers or quantum dots embedded on fiber-based functional SA devices that capable to generate ultrashort pulses. However, there is no reported study investigating different BP structures-SA in fixed fiber laser configuration towards their pulse performance.

Besides that, there are weaknesses in commonly reported deposition techniques, which are based on optical deposition, sandwiching, and wrapping method to transfer the mono or few-layer BP material onto fiber-based devices. For optical deposition method, it often requires precise control of the light output power to deposit material on the fiber surface. The uniformity of material deposition is still questionable in this method. Because of that, optimization of light output power is required for each different material in solution. Besides this technique, the sandwiching method is often reported in depositing material or thin film between two fiber ferrules platform. The drawback of this method is uncontrollable thickness of material deposited on the core where several trials and adjustment of materials thickness were needed to produce short pulses. Whereas for thin film placement, it required high technical skill and practice to place the tiny film on the core without any folding. Furthermore, this type of SA has low thermal damage threshold because the deposited materials interact with the highest intensity of light directly at the center of the fiber core. Next, the wrapping method is also performed on microfiber platform with material composite (thin film substrate). This method is complex and difficult to handle. In fact, there is possibility of material-wrapped gap in between microfiber. Hence, the pulse performance will be affected. Overall, all these methods are either difficult to control or scale up in production. In addition, optimized materials-based microfiber-SAs has not been reported from the perspective of microfiber dimension. The only related investigation was study on CNT based material with different waist diameter microfiber towards pulse performance [23].

In summary, none of the mentioned techniques above offer an exact fair ground to compare pulse performance of different BP dimension incorporated onto the same SA. It is important to understand the differences to improve the techniques for scalable and repeatable fabrication.

1.3 Aim and Objective

- I. To synthesize and characterize different BP structures via liquid phase exfoliation method,
- II. To optimize spin coating parameters and microfiber dimensions of BP-based SA for shortest pulse duration,
- III. To fabricate SA coated with varied BP structure based on optimized parameters as attained in Objective II, and
- IV. To compare with other BP SA on ultrashort pulse laser performance.

1.4 Scope of Work

The scope of work in this research is outlined in Figure 1.1, where the highlighted subsets are the focus of this research.

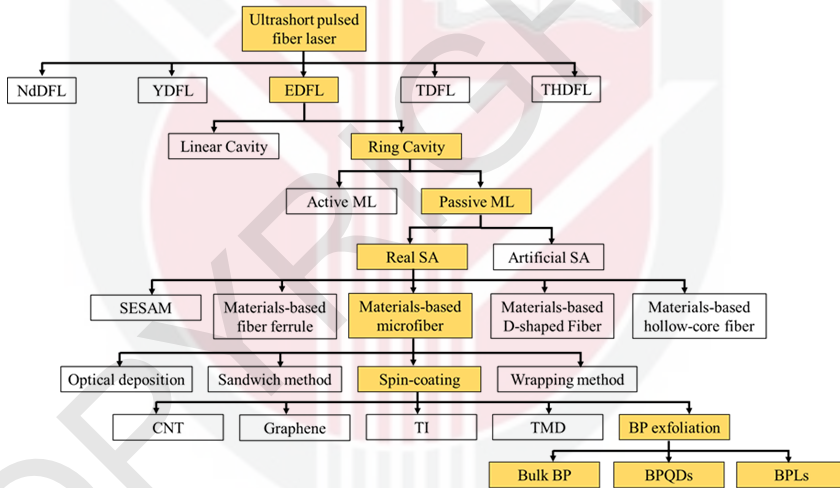


Figure 1.1: Scope of Work.

In this research, ring-type EDFL setup is selected for ultrashort pulse generation due to its well understood mechanism. Next, passive mode-locking technique based on real SAs is selected as it allows greater control of pulse performance against environmental perturbation as experienced by artificial SAs. For the real SAs, a microfiber is chosen as integrated structure due to its simplicity and strong evanescent field for light matter interaction at the tapered region. Before the microfiber is coated, optimization of microfiber dimensions and spin coating are investigated. In this work, BP material is mixed with polydimethylsiloxane (PDMS) before incorporated onto microfiber. Different structures of BP, black phosphorus layers (BPLs), and black phosphorus quantum dots (BPQDs) are synthesized and integrated as SA for better comparison in pulse generation.

Overall, the main focus of this work is to explore new and repeatable fabrication technique of BP-polymer microfiber SA that can provide a stable pulse laser source. The performance of mode-locking at 1.56 μm wavelength region will be discussed thoroughly in terms of spectral bandwidth, center wavelength, repetition rate, signal-to-noise ratio, pulse width, pulse energy and stability of the fiber laser system.

1.5 Organization of Thesis

The dissertation is organized as follows:

Chapter 1 consists of overview of ultrashort pulse laser, specifically on passively mode-locked fiber lasers. Issues with passive mode locking fiber laser are highlighted as well as the aim and objectives formed from those issues. The scope of work and thesis organization are also included in this chapter.

Chapter 2 presents the experimental and theoretical background of ultrashort pulse laser. This includes the mechanism of laser, effects of pulse propagation in optical fibers, soliton formation, and innovative fabrication techniques in the generation of mode-locked fiber lasers. In addition, optical properties of BP and its composite are also discussed. A critical review of reported BP-SAs passively mode-locked laser is also tabularized.

Chapter 3 demonstrates the experimental works of different dimension of BP-SA and few characterization tests are presented as supporting evidence for the generation of mode locking. This includes details of mode-locking performance from an optimized BP-SA.

Chapter 4 introduces the experimental synthesise of BP layers and BPQDs. Both BP structures are embedded on microfiber functions as SA for femtosecond pulse generations investigation. All the findings are discussed and analyzed.

Lastly, Chapter 5 concludes the main achievements of the research work. Recommendations for possible future investigation are suggested.

REFERENCES

- [1] Soong, H. K., & Malta, J. B. (2009). Femtosecond lasers in ophthalmology. *American journal of ophthalmology*, 147(2), 189-197.
- [2] Fermann, M. E., & Hartl, I. (2013). Ultrafast fibre lasers. *Nature photonics*, 7(11), 868-874.
- [3] Gattass, R. R., & Mazur, E. (2008). Femtosecond laser micromachining in transparent materials. *Nature photonics*, 2(4), 219-225.
- [4] de Vivie-Riedle, R., & Troppmann, U. (2007). Femtosecond lasers for quantum information technology. *Chemical reviews*, 107(11), 5082-5100.
- [5] Diddams, S. A., Hollberg, L., & Mbele, V. (2007). Molecular fingerprinting with the resolved modes of a femtosecond laser frequency comb. *Nature*, 445(7128), 627-630.
- [6] Xu, C., & Wise, F. W. (2013). Recent advances in fibre lasers for nonlinear microscopy. *Nature photonics*, 7(11), 875-882.
- [7] Lei, S., Zhao, X., Yu, X., Hu, A., Vukelic, S., Jun, M. B., Joe, H. E., Yao, Y. L., & Shin, Y. C. (2020). Ultrafast laser applications in manufacturing processes: a state-of-the-art review. *Journal of Manufacturing Science and Engineering*, 142(3), 031005.
- [8] Liu, X., Yao, X., & Cui, Y. (2018). Real-time observation of the buildup of soliton molecules. *Physical review letters*, 121(2), 023905.
- [9] Liu, X., & Cui, Y. (2019). Revealing the behavior of soliton buildup in a mode-locked laser. *Advanced Photonics*, 1(1), 016003.
- [10] Yamashita, S. (2011). A tutorial on nonlinear photonic applications of carbon nanotube and graphene. *Journal of lightwave technology*, 30(4), 427-447.
- [11] Liang, L., Wang, J., Lin, W., Sumpter, B. G., Meunier, V., & Pan, M. (2014). Electronic bandgap and edge reconstruction in phosphorene materials. *Nano letters*, 14(11), 6400-6406.
- [12] Martinez, A., Xu, B., & Yamashita, S. (2014). Nanotube based nonlinear fiber devices for fiber lasers. *IEEE Journal of Selected Topics in Quantum Electronics*, 20(5), 89-98.
- [13] Hussain, S. A. (2019). comparison of Graphene and carbon nanotube Saturable Absorbers for Wavelength and pulse Duration tunability. *Scientific reports*, 9(1), 1-9.

- [14] Jasik, A., Muszalski, J., Pierściński, K., Bugajski, M., Talalaev, V. G., & Kosmala, M. (2009). Low-temperature grown near surface semiconductor saturable absorber mirror: Design, growth conditions, characterization, and mode-locked operation. *Journal of Applied Physics*, 106(5), 053101.
- [15] Ahmed, M. H. M., Ali, N. M., Salleh, Z. S., Rahman, A. A., Harun, S. W., Manaf, M., & Arof, H. (2014). All fiber mode-locked Erbium-doped fiber laser using single-walled carbon nanotubes embedded into polyvinyl alcohol film as saturable absorber. *Optics & Laser Technology*, 62, 40-43.
- [16] Huang, P. L., Lin, S. C., Yeh, C. Y., Kuo, H. H., Huang, S. H., Lin, G. R., ... & Cheng, W. H. (2012). Stable mode-locked fiber laser based on CVD fabricated graphene saturable absorber. *Optics express*, 20(3), 2460-2465.
- [17] Bernard, F., Zhang, H., Gorza, S. P., & Emplit, P. (2012, June). Towards mode-locked fiber laser using topological insulators. In *Nonlinear Photonics* (pp. NTh1A-5). Optical Society of America.
- [18] Mohanraj, J., Velmurugan, V., & Sivabalan, S. (2016). Transition metal dichalcogenides based saturable absorbers for pulsed laser technology. *Optical Materials*, 60, 601-617.
- [19] Park, K., Lee, J., Lee, Y. T., Choi, W. K., Lee, J. H., & Song, Y. W. (2015). Black phosphorus saturable absorber for ultrafast mode-locked pulse laser via evanescent field interaction. *Annalen der Physik*, 527(11-12), 770-776.
- [20] Jhon, Y. I., Koo, J., Anasori, B., Seo, M., Lee, J. H., Gogotsi, Y., & Jhon, Y. M. (2017). Metallic MXene saturable absorber for femtosecond mode-locked lasers. *Advanced Materials*, 29(40), 1702496.
- [21] Song, Y., Liang, Z., Jiang, X., Chen, Y., Li, Z., Lu, L., ... & Zhang, H. (2017). Few-layer antimonene decorated microfiber: ultra-short pulse generation and all-optical thresholding with enhanced long term stability. *2D Materials*, 4(4), 045010.
- [22] Guo, B., Wang, S. H., Wu, Z. X., Wang, Z. X., Wang, D. H., Huang, H., ... & Zhang, H. (2018). Sub-200 fs soliton mode-locked fiber laser based on bismuthene saturable absorber. *Optics express*, 26(18), 22750-22760.
- [23] Martinez, A., Al Araimi, M., Dmitriev, A., Lutsyk, P., Li, S., Mou, C., ... & Turitsyn, S. (2017). Low-loss saturable absorbers based on tapered fibers embedded in carbon nanotube/polymer composites. *APL Photonics*, 2(12), 126103.
- [24] Flichy, P. (1993). The Birth of Long Distance Communication. Semaphore Telegraphs in Europe (1790-1840). *Réseaux. Communication-Technologie-Société*, 1(1), 81-101.
- [25] Comtois, P. (2001). John Tyndall and the floating matter of the air. *Aerobiologia*, 17(3), 193-202.

- [26] Kaunitz, J. D. (2014). The fruits of fiber: the invention of the flexible fiberoptic gastroscope. *Digestive diseases and sciences*, 59(11), 2616-2618.
- [27] Likourezos, G. (1992). Jan. 28, 1958: A laser is born. *IEEE Spectrum*, 29(5), 43.
- [28] Mulvaney, W. P., & Beck, C. W. (1968). The laser beam in urology. *The Journal of urology*, 99(1), 112-115.
- [29] Wieneke, S., & Gerhard, C. (2018). *Lasers in Medical Diagnosis and Therapy*. IOP Publishing, Bristol, UK.
- [30] Svelto, O., & Hanna, D. C. (1998). *Principles of lasers* (Vol. 4). New York: Plenum press.
- [31] Pearsall, T. P. (2017). *Quantum photonics*. Springer.
- [32] Jelinkova, H., & Sulc, J. (2013). Laser characteristics. In *Lasers for Medical Applications* (pp. 17-46). Woodhead Publishing.
- [33] Galvanauskas, A. (2004). High power fiber lasers. *Optics and photonics news*, 15(7), 42-47.
- [34] Becker, P. M., Olsson, A. A., & Simpson, J. R. (1999). *Erbium-doped fiber amplifiers: fundamentals and technology*. Elsevier.
- [35] Koechner, W., & Bass, M. (2006). *Solid-state lasers: a graduate text*. Springer Science & Business Media.
- [36] Paschotta, R. (2008). *Field guide to laser pulse generation* (Vol. 14). Bellingham: SPIE press.
- [37] Pinto, A. N., André, P. S., Pinto, J. L., & da Rocha, F. Short optical pulses generation by gain switching of a DFB laser diode. *Confetele*, 99, 182.
- [38] Iwakuni, K., Inaba, H., Nakajima, Y., Kobayashi, T., Hosaka, K., Onae, A., & Hong, F. L. (2012). Narrow linewidth comb realized with a mode-locked fiber laser using an intra-cavity waveguide electro-optic modulator for high-speed control. *Optics express*, 20(13), 13769-13776.
- [39] Donin, V. I., Yakovin, D. V., & Gribanov, A. V. (2012). Diode-pumped green Nd: YAG laser with Q-switch and mode locking. *Optics letters*, 37(3), 338-340.
- [40] Maker, G. T., & Ferguson, A. I. (1989). Frequency-modulation mode locking of a diode-pumped Nd: YAG laser. *Optics letters*, 14(15), 788-790.
- [41] Ismail, M. A., Harun, S. W., Ahmad, H., & Paul, M. C. (2016). *Passive Q-switched and Mode-locked Fiber Lasers Using Carbon-based Saturable Absorbers*. IntechOpen.
- [42] Webster, A. (1964). *Useful Mathematical Formulas for Transform Limited Pulses*.

- [43] Lin, Y. H., Lo, J. Y., Tseng, W. H., Wu, C. I., & Lin, G. R. (2013). Self-amplitude and self-phase modulation of the charcoal mode-locked erbium-doped fiber lasers. *Optics express*, 21(21), 25184-25196.
- [44] Lee, H., Kwon, W. S., Kim, J. H., Kang, D., & Kim, S. (2015). Polarization insensitive graphene saturable absorbers using etched fiber for highly stable ultrafast fiber lasers. *Optics express*, 23(17), 22116-22122.
- [45] Kuriakose, V. C., & Porsezian, K. (2010). Elements of optical solitons: An overview. *Resonance*, 15(7), 643-666.
- [46] Walmsley, I., Waxer, L., & Dorrer, C. (2001). The role of dispersion in ultrafast optics. *Review of Scientific Instruments*, 72(1), 1-29.
- [47] Chiang, K. S., Chow, Y. T., Richardson, D. J., Taverner, D., Dong, L., Reekie, L., & Lo, K. M. (1997). Experimental demonstration of intermodal dispersion in a two-core optical fibre. *Optics communications*, 143(4-6), 189-192.
- [48] Agrawal, G. P. (2000). Nonlinear fiber optics. In *Nonlinear Science at the Dawn of the 21st Century* (pp. 195-211). Springer, Berlin, Heidelberg.
- [49] Singh, S., & Singh, N. (2007). Nonlinear effects in optical fibers: origin, management and applications. *progress in Electromagnetics Research*, 73, 249-275.
- [50] Fellegara, A., Artiglia, M., Andreassen, S. B., Melloni, A., Espunes, F. P., & Wabnitz, S. (1997). COST 241 intercomparison of nonlinear refractive index measurements in dispersion shifted optical fibres at $\lambda = 1550$ nm. *Electronics Letters*, 33(13), 1168-1170.
- [51] Bullough, R. K., & Caudrey, P. J. (1980). The soliton and its history. In *Solitons* (pp. 1-64). Springer, Berlin, Heidelberg.
- [52] Shabat, A., & Zakharov, V. (1972). Exact theory of two-dimensional self-focusing and one-dimensional self-modulation of waves in nonlinear media. *Soviet physics JETP*, 34(1), 62.
- [53] Hasegawa, A., & Tappert, F. (1973). Transmission of stationary nonlinear optical pulses in dispersive dielectric fibers. I. Anomalous dispersion. *Applied Physics Letters*, 23(3), 142-144.
- [54] Mollenauer, L. F., Stolen, R. H., & Gordon, J. P. (1980). Experimental observation of picosecond pulse narrowing and solitons in optical fibers. *Physical Review Letters*, 45(13), 1095.
- [55] François, P. L. (1991). Nonlinear propagation of ultrashort pulses in optical fibers: total field formulation in the frequency domain. *JOSA B*, 8(2), 276-293.
- [56] University of Dundee. Department of Mathematics, Griffiths, D. F., Mitchell, A. R., & Morris, J. L. (1982). *A numerical study of the nonlinear Schrödinger equation*.

- [57] Radhakrishnan, R., & Lakshmanan, M. (1995). Bright and dark soliton solutions to coupled nonlinear Schrodinger equations. *Journal of Physics A: Mathematical and General*, 28(9), 2683.
- [58] Efremidis, N. K., & Christodoulides, D. N. (2003). Discrete Ginzburg-Landau solitons. *Physical Review E*, 67(2), 026606.
- [59] Cui, Y., & Liu, X. (2013). Graphene and nanotube mode-locked fiber laser emitting dissipative and conventional solitons. *Optics express*, 21(16), 18969-18974.
- [60] Quraishi, Q., Cundiff, S. T., Ilan, B., & Ablowitz, M. J. (2005). Dynamics of nonlinear and dispersion managed solitons. *Physical review letters*, 94(24), 243904.
- [61] Grellu, P., & Akhmediev, N. (2012). Dissipative solitons for mode-locked lasers. *Nature photonics*, 6(2), 84-92.
- [62] Sun, Z., Rozhin, A. G., Wang, F., Hasan, T., Popa, D., O'neill, W., & Ferrari, A. C. (2009). A compact, high power, ultrafast laser mode-locked by carbon nanotubes. *Applied Physics Letters*, 95(25), 253102.
- [63] Xia, H., Li, H., Deng, G., Li, J., Zhang, S., & Liu, Y. (2015). Compact noise-like pulse fiber laser and its application for supercontinuum generation in highly nonlinear fiber. *Applied optics*, 54(32), 9379-9384.
- [64] You, Y. J., Wang, C., Lin, Y. L., Zaytsev, A., Xue, P., & Pan, C. L. (2015). Ultrahigh-resolution optical coherence tomography at 1.3 μm central wavelength by using a supercontinuum source pumped by noise-like pulses. *Laser Physics Letters*, 13(2), 025101.
- [65] Chen, H., Li, L., Ruan, S., Guo, T., & Yan, P. (2016). Fiber-integrated tungsten disulfide saturable absorber (mirror) for pulsed fiber lasers. *Optical Engineering*, 55(8), 081318.
- [66] Matsas, V. J., Newson, T. P., Richardson, D. J., & Payne, D. N. (1992). Self-starting passively mode-locked fibre ring soliton laser exploiting nonlinear polarisation rotation. *Electronics Letters*, 28(15), 1391-1393.
- [67] Xiu-Jiang, H., Zhan, S., Yong-Zhi, L., Ming-Zhong, L., Hong-Huan, L., Jian-Jun, W., ... & Hai-Yan, C. (2005). Research on highly Yb³⁺-doped passive mode-locked fiber ring laser. *Microwave and Optical Technology Letters*, 45(3), 269-270.
- [68] Gao, C., Wang, Z., Luo, H., & Zhan, L. (2017). High energy all-fiber Tm-doped femtosecond soliton laser mode-locked by nonlinear polarization rotation. *Journal of Lightwave Technology*, 35(14), 2988-2993.
- [69] Tan, S. J., Tiu, Z. C., Harun, S. W., & Ahmad, H. (2015). Sideband-controllable soliton pulse with bismuth-based erbium-doped fiber. *Chinese Optics Letters*, 13(11), 111406.

- [70] Tang, D. Y., Zhao, B., Zhao, L. M., & Tam, H. Y. (2005). Soliton interaction in a fiber ring laser. *Physical Review E*, 72(1), 016616.
- [71] Akhmediev, N., Soto-Crespo, J. M., Grapinet, M., & Grelu, P. (2005). Dissipative soliton interactions inside a fiber laser cavity. *Optical Fiber Technology*, 11(3), 209-228.
- [72] Grelu, P., & Soto-Crespo, J. M. (2004). Multisoliton states and pulse fragmentation in a passively mode-locked fibre laser. *Journal of Optics B: Quantum and Semiclassical Optics*, 6(5), S271.
- [73] Tang, D. Y., Zhao, L. M., Zhao, B., & Liu, A. Q. (2005). Mechanism of multisoliton formation and soliton energy quantization in passively mode-locked fiber lasers. *Physical Review A*, 72(4), 043816.
- [74] Nelson, L. E., Jones, D. J., Tamura, K., Haus, H. A., & Ippen, E. P. (1997). Ultrashort-pulse fiber ring lasers. *Applied Physics B: Lasers & Optics*, 65(2).
- [75] Luo, J. L., Li, L., Ge, Y. Q., Jin, X. X., Tang, D. Y., Zhang, S. M., & Zhao, L. M. (2014). L -Band Femtosecond Fiber Laser Mode Locked by Nonlinear Polarization Rotation. *IEEE Photonics Technology Letters*, 26(24), 2438-2441.
- [76] Mahmoodi, S., Bacher, C., Heidt, A., Lätt, C., Abdollahpour, D., Romano, V., ... & Ryser, M. (2021). Ultrashort pulse formation from a thulium-doped fiber laser: Self-characterization and mapping. *Optics communications*, 486, 126747.
- [77] Huang, L., Zhang, Y., & Liu, X. (2020). Dynamics of carbon nanotube-based mode-locking fiber lasers. *Nanophotonics*, 9(9), 2731-2761.
- [78] Wu, X., Tang, D. Y., Zhao, L. M., & Zhang, H. (2010). Mode-Locking of fiber lasers induced by residual polarization dependent loss of cavity components. *Laser physics*, 20(10), 1913-1917.
- [79] Keller, U., Weingarten, K. J., Kartner, F. X., Kopf, D., Braun, B., Jung, I. D., ... & Der Au, J. A. (1996). Semiconductor saturable absorber mirrors (SESAM's) for femtosecond to nanosecond pulse generation in solid-state lasers. *IEEE Journal of selected topics in QUANTUM ELECTRONICS*, 2(3), 435-453.
- [80] Schön, S., Haiml, M., & Keller, U. (2000). Ultrabroadband AlGaAs/CaF₂ semiconductor saturable absorber mirrors. *Applied Physics Letters*, 77(6), 782-784.
- [81] Schmidt, A., Rivier, S., Cho, W. B., Yim, J. H., Choi, S. Y., Lee, S., ... & Griebner, U. (2009). Sub-100 fs single-walled carbon nanotube saturable absorber mode-locked Yb-laser operation near 1 μm . *Optics express*, 17(22), 20109-20116.

- [82] Dong, B., Liaw, C. Y., Hao, J., & Hu, J. (2010). Nanotube Q-switched low-threshold linear cavity tunable erbium-doped fiber laser. *Applied Optics*, 49(31), 5989-5992.
- [83] Lau, K. Y., Ng, E. K., Bakar, M. A., Abas, A. F., Alresheedi, M. T., Yusoff, Z., & Mahdi, M. A. (2018). Low threshold linear cavity mode-locked fiber laser using microfiber-based carbon nanotube saturable absorber. *Optics & Laser Technology*, 102, 240-246.
- [84] Martinez, A., Fuse, K., & Yamashita, S. (2011). Mechanical exfoliation of graphene for the passive mode-locking of fiber lasers. *Applied Physics Letters*, 99(12), 121107.
- [85] Chen, Y. L., Analytis, J. G., Chu, J. H., Liu, Z. K., Mo, S. K., Qi, X. L., ... & Shen, Z. X. (2009). Experimental realization of a three-dimensional topological insulator, Bi₂Te₃. *science*, 325(5937), 178-181.
- [86] Wang, S., Yu, H., Zhang, H., Wang, A., Zhao, M., Chen, Y., ... & Wang, J. (2014). Broadband few-layer MoS₂ saturable absorbers. *Advanced materials*, 26(21), 3538-3544.
- [87] Li, D., Jussila, H., Karvonen, L., Ye, G., Lipsanen, H., Chen, X., & Sun, Z. (2015). Polarization and thickness dependent absorption properties of black phosphorus: new saturable absorber for ultrafast pulse generation. *Scientific reports*, 5(1), 1-9.
- [88] Boyd, R. W. (2020). *Nonlinear optics*. Academic press.
- [89] Jeon, J., Lee, J., & Lee, J. H. (2015). Numerical study on the minimum modulation depth of a saturable absorber for stable fiber laser mode locking. *JOSA B*, 32(1), 31-37.
- [90] Lou, F., Cui, L., Li, Y. B., Hou, J., He, J. L., Jia, Z. T., ... & Tao, X. T. (2013). High-efficiency femtosecond Yb: Gd₃Al_{0.5}Ga_{4.5}O₁₂ mode-locked laser based on reduced graphene oxide. *Optics letters*, 38(20), 4189-4192.
- [91] Xu, J. L., Li, X. L., Wu, Y. Z., Hao, X. P., He, J. L., & Yang, K. J. (2011). Graphene saturable absorber mirror for ultra-fast-pulse solid-state laser. *Optics letters*, 36(10), 1948-1950.
- [92] Xu, J., Liu, J., Wu, S., Yang, Q. H., & Wang, P. (2012). Graphene oxide mode-locked femtosecond erbium-doped fiber lasers. *Optics express*, 20(14), 15474-15480.
- [93] Xu, J., Wu, S., Li, H., Liu, J., Sun, R., Tan, F., ... & Wang, P. (2012). Dissipative soliton generation from a graphene oxide mode-locked Er-doped fiber laser. *Optics express*, 20(21), 23653-23658.
- [94] Zhang, M., Kelleher, E. J. R., Torrisi, F., Sun, Z., Hasan, T., Popa, D., ... & Taylor, J. R. (2012). Tm-doped fiber laser mode-locked by graphene-polymer composite. *Optics express*, 20(22), 25077-25084.

- [95] Liu, H., Zheng, X. W., Liu, M., Zhao, N., Luo, A. P., Luo, Z. C., ... & Wen, S. C. (2014). Femtosecond pulse generation from a topological insulator mode-locked fiber laser. *Optics express*, 22(6), 6868-6873.
- [96] Sotor, J., Sobon, G., Macherzynski, W., Paletko, P., Grodecki, K., & Abramski, K. M. (2014). Mode-locking in Er-doped fiber laser based on mechanically exfoliated Sb₂Te₃ saturable absorber. *Optical materials express*, 4(1), 1-6.
- [97] Jung, M., Koo, J., Chang, Y. M., Debnath, P., Song, Y. W., & Lee, J. H. (2012). An all fiberized, 1.89- μ m Q-switched laser employing carbon nanotube evanescent field interaction. *Laser Physics Letters*, 9(9), 669.
- [98] Song, Y. W., Yamashita, S., Goh, C. S., & Set, S. Y. (2007). Carbon nanotube mode lockers with enhanced nonlinearity via evanescent field interaction in D-shaped fibers. *Optics letters*, 32(2), 148-150.
- [99] Im, J. H., Choi, S. Y., Rotermund, F., & Yeom, D. I. (2010). All-fiber Er-doped dissipative soliton laser based on evanescent field interaction with carbon nanotube saturable absorber. *Optics express*, 18(21), 22141-22146.
- [100] Kashiwagi, K., & Yamashita, S. (2009). Deposition of carbon nanotubes around microfiber via evanescent light. *Optics express*, 17(20), 18364-18370.
- [101] Kieu, K., & Mansuripur, M. (2007). Femtosecond laser pulse generation with a fiber taper embedded in carbon nanotube/polymer composite. *Optics letters*, 32(15), 2242-2244.
- [102] Shohda, F., Shirato, T., Nakazawa, M., Komatsu, K., & Kaino, T. (2008). A passively mode-locked femtosecond soliton fiber laser at 1.5 μ m with a CNT-doped polycarbonate saturable absorber. *Optics express*, 16(26), 21191-21198.
- [103] Liu, M., Zheng, X. W., Qi, Y. L., Liu, H., Luo, A. P., Luo, Z. C., ... & Zhang, H. (2014). Microfiber-based few-layer MoS₂ saturable absorber for 2.5 GHz passively harmonic mode-locked fiber laser. *Optics express*, 22(19), 22841-22846.
- [104] Choi, S. Y., Cho, D. K., Song, Y. W., Oh, K., Kim, K., Rotermund, F., & Yeom, D. I. (2012). Graphene-filled hollow optical fiber saturable absorber for efficient soliton fiber laser mode-locking. *Optics express*, 20(5), 5652-5657.
- [105] Liu, Z. B., He, X., & Wang, D. N. (2011). Passively mode-locked fiber laser based on a hollow-core photonic crystal fiber filled with few-layered graphene oxide solution. *Optics letters*, 36(16), 3024-3026.
- [106] Yan, P., Liu, A., Chen, Y., Wang, J., Ruan, S., Chen, H., & Ding, J. (2015). Passively mode-locked fiber laser by a cell-type WS₂ nanosheets saturable absorber. *Scientific reports*, 5(1), 1-7.

- [107] Jung, M., Lee, J., Park, J., Koo, J., Jhon, Y. M., & Lee, J. H. (2015). Mode-locked, 1.94- μm , all-fiberized laser using WS_2 -based evanescent field interaction. *Optics express*, 23(15), 19996-20006.
- [108] Song, Y. W., Jang, S. Y., Han, W. S., & Bae, M. K. (2010). Graphene mode-lockers for fiber lasers functioned with evanescent field interaction. *Applied Physics Letters*, 96(5), 051122.
- [109] Khazaeinezhad, R., Kassani, S. H., Jeong, H., Park, K. J., Kim, B. Y., Yeom, D. I., & Oh, K. (2015). Ultrafast pulsed all-fiber laser based on tapered fiber enclosed by few-layer WS_2 nanosheets. *IEEE Photonics Technology Letters*, 27(15), 1581-1584.
- [110] Luo, Z. C., Cao, W. J., Luo, A. P., Xu, W. C., & Xu, W. C. (2012). Optical deposition of graphene saturable absorber integrated in a fiber laser using a slot collimator for passive mode-locking. *Applied Physics Express*, 5(5), 055103.
- [111] Khazaeizhad, R., Kassani, S. H., Jeong, H., Yeom, D. I., & Oh, K. (2014). Mode-locking of Er-doped fiber laser using a multilayer MoS_2 thin film as a saturable absorber in both anomalous and normal dispersion regimes. *Optics express*, 22(19), 23732-23742.
- [112] Nishizawa, N., Seno, Y., Sumimura, K., Sakakibara, Y., Itoga, E., Kataura, H., & Itoh, K. (2008). All-polarization-maintaining Er-doped ultrashort-pulse fiber laser using carbon nanotube saturable absorber. *Optics express*, 16(13), 9429-9435.
- [113] Xia, H., Li, H., Lan, C., Li, C., Zhang, X., Zhang, S., & Liu, Y. (2014). Ultrafast erbium-doped fiber laser mode-locked by a CVD-grown molybdenum disulfide (MoS_2) saturable absorber. *Optics express*, 22(14), 17341-17348.
- [114] Zhang, M., Howe, R. C., Woodward, R. I., Kelleher, E. J., Torrisi, F., Hu, G., ... & Hasan, T. (2015). Solution processed MoS_2 -PVA composite for sub-bandgap mode-locking of a wideband tunable ultrafast Er: fiber laser. *Nano Research*, 8(5), 1522-1534.
- [115] Cui, Y., Lu, F., & Liu, X. (2016). MoS_2 -clad microfiber laser delivering conventional, dispersion-managed and dissipative solitons. *Scientific reports*, 6(1), 1-8.
- [116] Liu, X. M., Yang, H. R., Cui, Y. D., Chen, G. W., Yang, Y., Wu, X. Q., ... & Tong, L. M. (2016). Graphene-clad microfiber saturable absorber for ultrafast fibre lasers. *Scientific reports*, 6(1), 1-8.
- [117] Liu, H., Neal, A. T., Zhu, Z., Luo, Z., Xu, X., Tománek, D., & Ye, P. D. (2014). Phosphorene: an unexplored 2D semiconductor with a high hole mobility. *ACS nano*, 8(4), 4033-4041.

- [118] Xia, F., Wang, H., & Jia, Y. (2014). Rediscovering black phosphorus as an anisotropic layered material for optoelectronics and electronics. *Nature communications*, 5(1), 1-6.
- [119] Xin, C., Zheng, J., Su, Y., Li, S., Zhang, B., Feng, Y., & Pan, F. (2016). Few-layer tin sulfide: a new black-phosphorus-analogue 2D material with a sizeable band gap, odd–even quantum confinement effect, and high carrier mobility. *The Journal of Physical Chemistry C*, 120(39), 22663-22669.
- [120] Lan, S., Rodrigues, S., Kang, L., & Cai, W. (2016). Visualizing optical phase anisotropy in black phosphorus. *Acs Photonics*, 3(7), 1176-1181.
- [121] Tran, V., Soklaski, R., Liang, Y., & Yang, L. (2014). Layer-controlled band gap and anisotropic excitons in few-layer black phosphorus. *Physical Review B*, 89(23), 235319.
- [122] Low, T., Rodin, A. S., Carvalho, A., Jiang, Y., Wang, H., Xia, F., & Neto, A. C. (2014). Tunable optical properties of multilayer black phosphorus thin films. *Physical Review B*, 90(7), 075434.
- [123] Wang, X., & Lan, S. (2016). Optical properties of black phosphorus. *Advances in Optics and photonics*, 8(4), 618-655.
- [124] Chen, Y., Jiang, G., Chen, S., Guo, Z., Yu, X., Zhao, C., ... & Fan, D. (2015). Mechanically exfoliated black phosphorus as a new saturable absorber for both Q-switching and mode-locking laser operation. *Optics express*, 23(10), 12823-12833.
- [125] Niu, L., Coleman, J. N., Zhang, H., Shin, H., Chhowalla, M., & Zheng, Z. (2016). Production of two-dimensional nanomaterials via liquid-based direct exfoliation. *Small*, 12(3), 272-293.
- [126] Sinha, S., Takabayashi, Y., Shinohara, H., & Kitaura, R. (2016). Simple fabrication of air-stable black phosphorus heterostructures with large-area hBN sheets grown by chemical vapor deposition method. *2D Materials*, 3(3), 035010.
- [127] Wang, K., Szydłowska, B. M., Wang, G., Zhang, X., Wang, J. J., Magan, J. J., ... & Blau, W. J. (2016). Ultrafast nonlinear excitation dynamics of black phosphorus nanosheets from visible to mid-infrared. *ACS nano*, 10(7), 6923-6932.
- [128] Lu, S. B., Miao, L. L., Guo, Z. N., Qi, X., Zhao, C. J., Zhang, H., ... & Fan, D. Y. (2015). Broadband nonlinear optical response in multi-layer black phosphorus: an emerging infrared and mid-infrared optical material. *Optics express*, 23(9), 11183-11194.
- [129] Margulis, V. A., Muryumin, E. E., & Gaiduk, E. A. (2018). Optical Kerr effect and two-photon absorption in monolayer black phosphorus. *Journal of Optics*, 20(5), 055503.

- [130] Zhang, F., Wu, Z., Wang, Z., Wang, D., Wang, S., & Xu, X. (2016). Strong optical limiting behavior discovered in black phosphorus. *RSC advances*, 6(24), 20027-20033.
- [131] Kim, J. H., Lau, K. T., Shepherd, R., Wu, Y., Wallace, G., & Diamond, D. (2008). Performance characteristics of a polypyrrole modified polydimethylsiloxane (PDMS) membrane based microfluidic pump. *Sensors and Actuators A: Physical*, 148(1), 239-244.
- [132] Lin, Y. H., Kang, S. W., & Wu, T. Y. (2009). Fabrication of polydimethylsiloxane (PDMS) pulsating heat pipe. *Applied Thermal Engineering*, 29(2-3), 573-580.
- [133] Yang, R., Yu, Y. S., Zhu, C. C., Xue, Y., Chen, C., Zhang, X. Y., ... & Sun, H. B. (2015). PDMS-coated S-tapered fiber for highly sensitive measurements of transverse load and temperature. *IEEE Sensors Journal*, 15(6), 3429-3435.
- [134] Fujii, T. (2002). PDMS-based microfluidic devices for biomedical applications. *Microelectronic Engineering*, 61, 907-914.
- [135] Na, D., Park, K., Park, K. H., & Song, Y. W. (2017). Passivation of black phosphorus saturable absorbers for reliable pulse formation of fiber lasers. *Nanotechnology*, 28(47), 475207.
- [136] Yu, H., Zheng, X., Yin, K., & Jiang, T. (2016). Nanosecond passively Q-switched thulium/holmium-doped fiber laser based on black phosphorus nanoplatelets. *Optical Materials Express*, 6(2), 603-609.
- [137] Pawlizewska, M., Ge, Y., Li, Z., Zhang, H., & Sotor, J. (2017). Fundamental and harmonic mode-locking at 2.1 μm with black phosphorus saturable absorber. *Optics Express*, 25(15), 16916-16921.
- [138] Chen, Y., Mu, H., Li, P., Lin, S., Nanjunda, S. B., & Bao, Q. (2016). Optically driven black phosphorus as a saturable absorber for mode-locked laser pulse generation. *Optical Engineering*, 55(8), 081317.
- [139] Li, L., Wang, Y., & Wang, X. (2017). Ultrafast pulse generation with black phosphorus solution saturable absorber. *Laser Physics*, 27(8), 085104.
- [140] Luo, Z. C., Liu, M., Guo, Z. N., Jiang, X. F., Luo, A. P., Zhao, C. J., ... & Zhang, H. (2015). Microfiber-based few-layer black phosphorus saturable absorber for ultra-fast fiber laser. *Optics express*, 23(15), 20030-20039.
- [141] Yu, H., Zheng, X., Yin, K., & Jiang, T. (2015). Thulium/holmium-doped fiber laser passively mode locked by black phosphorus nanoplatelets-based saturable absorber. *Applied optics*, 54(34), 10290-10294.
- [142] Chen, Yu, et al. "Sub-300 femtosecond soliton tunable fiber laser with all-anomalous dispersion passively mode locked by black phosphorus." *Optics Express* 24.12 (2016): 13316-13324.

- [143] Ravets, S., Hoffman, J. E., Kordell, P. R., Wong-Campos, J. D., Rolston, S. L., & Orozco, L. A. (2013). Intermodal energy transfer in a tapered optical fiber: optimizing transmission. *JOSA A*, 30(11), 2361-2371.
- [144] Love, J. D., Henry, W. M., Stewart, W. J., Black, R. J., Lacroix, S., & Gonthier, F. (1991). Tapered single-mode fibres and devices. Part 1: Adiabaticity criteria. *IEE Proceedings J (Optoelectronics)*, 138(5), 343-354.
- [145] Lee, H. U., Lee, S. C., Won, J., Son, B. C., Choi, S., Kim, Y., & Lee, J. (2015). Stable semiconductor black phosphorus (BP)@ titanium dioxide (TiO₂) hybrid photocatalysts. *Scientific reports*, 5(1), 1-6.
- [146] Surrente, A., Mitioglu, A. A., Galkowski, K., Tabis, W., Maude, D. K., & Plochocka, P. (2016). Excitons in atomically thin black phosphorus. *Physical Review B*, 93(12), 121405.
- [147] Chen, Y., Zhao, C., Chen, S., Du, J., Tang, P., Jiang, G., ... & Tang, D. (2013). Large energy, wavelength widely tunable, topological insulator Q-switched erbium-doped fiber laser. *IEEE Journal of Selected Topics in Quantum Electronics*, 20(5), 315-322.
- [148] Paschotta, R., & Keller, U. (2001). Passive mode locking with slow saturable absorbers. *Applied Physics B*, 73(7), 653-662.
- [149] Sobon, G., Sotor, J., Pasternak, I., Krajewska, A., Strupinski, W., & Abramski, K. M. (2015). Multilayer graphene-based saturable absorbers with scalable modulation depth for mode-locked Er-and Tm-doped fiber lasers. *Optical Materials Express*, 5(12), 2884-2894.
- [150] Hanlon, D., Backes, C., Doherty, E., Cucinotta, C. S., Berner, N. C., Boland, C., ... & Coleman, J. N. (2015). Liquid exfoliation of solvent-stabilized few-layer black phosphorus for applications beyond electronics. *Nature communications*, 6(1), 1-11.
- [151] Lee, M., Park, Y. H., Kang, E. B., Chae, A., Choi, Y., Jo, S., ... & In, I. (2017). Highly efficient visible blue-emitting black phosphorus quantum dot: Mussel-inspired surface functionalization for bioapplications. *ACS omega*, 2(10), 7096-7105.
- [152] Lewis, E. A., Brent, J. R., Derby, B., Haigh, S. J., & Lewis, D. J. (2017). Solution processing of two-dimensional black phosphorus. *Chemical Communications*, 53(9), 1445-1458.
- [153] Castellanos-Gomez, A., Vicarelli, L., Prada, E., Island, J. O., Narasimha-Acharya, K. L., Blanter, S. I., ... & Van Der Zant, H. S. (2014). Isolation and characterization of few-layer black phosphorus. *2D Materials*, 1(2), 025001.
- [154] Suryawanshi, S. R., More, M. A., & Late, D. J. (2016). Laser exfoliation of 2D black phosphorus nanosheets and their application as a field emitter. *RSC advances*, 6(113), 112103-112108.

- [155] Liang, S., Hasan, M. N., & Seo, J. H. (2019). Direct observation of Raman spectra in black phosphorus under uniaxial strain conditions. *Nanomaterials*, 9(4), 566.
- [156] Gui, R., Jin, H., Wang, Z., & Li, J. (2018). Black phosphorus quantum dots: synthesis, properties, functionalized modification and applications. *Chemical Society Reviews*, 47(17), 6795-6823.
- [157] Luo, Z., Li, Y., Zhong, M., Huang, Y., Wan, X., Peng, J., & Weng, J. (2015). Nonlinear optical absorption of few-layer molybdenum diselenide (MoSe₂) for passively mode-locked soliton fiber laser. *Photonics Research*, 3(3), A79-A86.
- [158] Dong, Z., Tian, J., Li, R., Cui, Y., Zhang, W., & Song, Y. (2020). Conventional Soliton and Noise-Like Pulse Generated in an Er-Doped Fiber Laser with Carbon Nanotube Saturable Absorbers. *Applied Sciences*, 10(16), 5536.
- [159] Chen, R., Zheng, X., & Jiang, T. (2017). Broadband ultrafast nonlinear absorption and ultra-long exciton relaxation time of black phosphorus quantum dots. *Optics express*, 25(7), 7507-7519.
- [160] Chen, B., Zhang, X., Wu, K., Wang, H., Wang, J., & Chen, J. (2015). Q-switched fiber laser based on transition metal dichalcogenides MoS₂, MoSe₂, WS₂, and WSe₂. *Optics express*, 23(20), 26723-26737.
- [161] Deng, Z.S., Zhao, G.K., Yuan, J.Q., Lin, J.P., Chen, H.J., Liu, H.Z., Luo, A.P., Cui, H., Luo, Z.C., & Xu, W.C. (2017). Switchable generation of rectangular noise-like pulse and dissipative soliton resonance in a fiber laser. *Optics Letters*, 42(21), 4517-4520.
- [162] Wu, C., Yao, Y., Wu, Q., Yang, Y., Tian, J. & Xu, K. (2021). Noise-like pulses under different intra-cavity nonlinearity. *Optical Fiber Technology*, 64, 102549.
- [163] Huang, J., Dong, N., Zhang, S., Sun, Z., Zhang, W. & Wang, J. (2017). Nonlinear absorption induced transparency and optical limiting of black phosphorus nanosheets. *ACS Photonics*, 4(12), 3063-3070.
- [164] Zhao, J., Zhou, J., Jiang, Y., Li, L., Shen, D., Komarov, A., Su, L., Tang, D., Klimczak, M. & Zhao, L. (2020). Nonlinear absorbing-loop mirror in a holmium-doped fiber laser. *Journal of Lightwave Technology*, 38(21), 6069-6075.
- [165] Voropaev, V., Donodin, A., Voronets, A., Vlasov, D., Lazarev, V., Tarabrin, M. & Krylov, A. (2019). Generation of multi-solitons and noise-like pulses in a high-powered thulium-doped all-fiber ring oscillator. *Scientific Reports*, 9(1), 1-11.
- [166] Cheng, Z., Li, H. & Wang, P. (2015). Simulation of generation of dissipative soliton, dissipative soliton resonance and noise-like pulse in Yb-doped mode-locked fiber lasers. *Optics Express*, 23(5), 5972-5981.